



Electrochemical Nonenzymatic Acetone Sensing: A Novel Approach of Biosensor Platform Based on CNT/CuO Nanosystems

Mithra Geetha, Gayathri Geetha Nair, Kishor Kumar Sadasivuni,* Somaya Al-maadeed, and Asan G. A. Muthalif

A promising approach for noninvasive medical diagnosis may be to measure the VOCs produced by metabolic changes or pathological disorders in human sweat, such as measuring the acetone levels in the presence of diabetes. Acetone is a by-product of fat catabolism and serves as an indicator of ketosis and diabetes. The measurement of acetone may be used instead of glucose monitoring. Current research aims to develop and improve noninvasive methods of detecting acetone in sweat that are accurate, sensitive, and stable. The carbon nanotubes (CNTs)–copper oxide (CuO) nanocomposite (NC) improves direct electron transport to the electrode surface in this study. The complex-precipitation method is used to make this NC. X-ray diffraction (XRD) and scanning electron microscopy (SEM) are used to investigate the crystal structure and morphology of the prepared catalyst. Using cyclic voltammetry (CV) and amperometry, the electrocatalytic activity of the as-prepared catalyst is evaluated. The electrocatalytic activity in artificial sweat solution is examined at various scan rates and acetone concentrations. The detection limit of the CNTs-CuO NC catalyst is 0.05 mM, with a sensitivity of 16.1 mA cm⁻² μM⁻¹ in a linear range of 1–50 mM. Furthermore, this NC demonstrates a high degree of selectivity for various biocompounds found in sweat, with no interfering cross-reactions from these species. The CNT-CuO NC, as produced, has good sensitivity, rapid reaction time (2 s), and stability, indicating its potential for acetone sensing.

metabolic condition of the individual. It is possible to use disease-specific VOCs as disease biomarkers. Novel therapeutic approaches for treating various diseases may be derived from the elucidation of pathophysiological mechanisms underlying the production of disease-specific VOCs. Sweat is a major source of VOCs emitted from the skin. Changes in the homeostatic balance area can affect both the quality and quantity of VOCs. A promising approach for noninvasive medical diagnosis may be to measure the VOCs produced by metabolic changes or pathological disorders in human sweat, such as measuring the acetone levels in the presence of diabetes.^[1] Acetone is a by-product of fat catabolism and serves as an indicator of ketosis, diabetes, a low carbohydrate diet, and weight loss. The measurement of acetone may be used instead of glucose monitoring. Fat consumption increases in cells under these physiological stresses, as do blood ketone levels. Acetone is the only ketone body that partitions effectively from the blood into sweat.^[2]

The low detection limit possible with electrochemical techniques opens the possibility of developing acetone detection

methods for human tissues and fluids other than blood. Electrochemical sensors have acquired popularity in quick diagnosis due to their low cost, ease of preparation, sensitivity, rapid

1. Introduction

Human body releases hundreds of volatile organic compounds (VOCs), and the components of VOCs generally reflect the

M. Geetha, K. K. Sadasivuni
Center for Advanced Materials
Qatar University
Doha 2713, Qatar
E-mail: chishorecumar@gmail.com

G. G. Nair
Amal Jyothi College of Engineering Kanjirappally
Koovappally P.O., Kottayam Dt., Thiruvananthapuram, Kerala India
S. Al-maadeed
Department of Computer Science and Engineering
Qatar University
Doha 2713, Qatar
A. G. A. Muthalif
Department of Mechanical and Industrial Engineering
Qatar University
Doha 2713, Qatar

The ORCID identification number(s) for the author(s) of this article can be found under <https://doi.org/10.1002/masy.202200150>

© 2023 The Authors. Macromolecular Symposia published by Wiley-VCH GmbH. This is an open access article under the terms of the Creative Commons Attribution License, which permits use, distribution and reproduction in any medium, provided the original work is properly cited.

DOI: 10.1002/masy.202200150

response, and simple operation that allows for individual self-monitoring.^[3] Because the electrode surface plays an essential role in fabricating nonenzymatic acetone detectors, synthesizing a catalyst with porous structures is critical. High active sites, high permeability, and a shorter charge transfer channel length are benefits of micro-/nanoporous morphologies, which are attractive for sensor applications.

Carbon nanotubes (CNTs) are made up of layers of carbon atoms organized in six-membered rings. Porosity is formed by an amorphous structure of aromatic sheets and strips with slits of varying molecular diameters. CNTs are made up of curved sp²-hybridized carbon atoms stacked in concentric cylindrical planes in an axial orientation.^[4] The oxygen functional groups on the supports have been important in defining their uses. On the other hand, CuO is a nontoxic n-type semiconductor compound with a narrow bandgap (1.21–1.51 eV), excellent permeation, high number of active sites, high surface area, and strong electrical characteristics that can improve the electrochemical properties of CNT. Furthermore, by synthesizing the NC of CNT and CuO, porous morphologies of the catalyst may be obtained. The NC creation produces a morphology with a high surface-to-volume ratio, which improves the material's electrocatalytic activity.^[5] The usage of CNTs in combination with CuO nanoparticles has been discovered to improve electron transport while the metallic centers carry out the catalysis. As a result, this study looked at the prospect of using CNT-coupled CuO's electrocatalytic nature for acetone testing.

This paper focuses on applying sweat acetone detection as a possible tool to monitor diabetes, as patients with diabetes tend to have higher acetone levels in their sweat than healthy people.^[6] Sweat acetone is considered one of the biomarkers of this disease and the aim in the future is to reduce the number of blood sugar measurements per day. The sweat acetone is usually in the range of 0.2–1.8 ppm for healthy people, and in the range of 1.25–2.5 ppm for people with diabetes.^[7] In order to measure such low gas concentrations in the laboratory, the systems mentioned above can be applied.

This study explores the possibility of using CNT-CuO as a catalytic interface for enzyme-free acetone measurement in an artificial sweat solution. The cyclic voltammetry (CV) response for various acetone concentrations was used to test the material's sensitivity. The synergistic consequence encouraged by electrical interactions among CNT/CuO NC plays a significant role in improving the electrocatalytic performance of this NC for efficient acetone detection. Electrodes made of CNT/CuO NC can be employed in wearable biosensors to monitor acetone levels in human sweat. Diabetes, atherosclerosis, diabetic retinopathy, renal failure, nerve degeneration, and other diseases can be reduced with proper acetone monitoring.

2. Results and Discussion

2.1. Structural and Morphological Analysis of CNTs/CuO NC

CNT is identified by diffraction spectra acquired by X-ray scattering. **Figure 1** shows the XRD patterns of as-synthesized CNTs/CuO NC. The CNTs/CuO NC validates the monoclinic CuO and cubic CNT phases based on XRD measurements^[7].

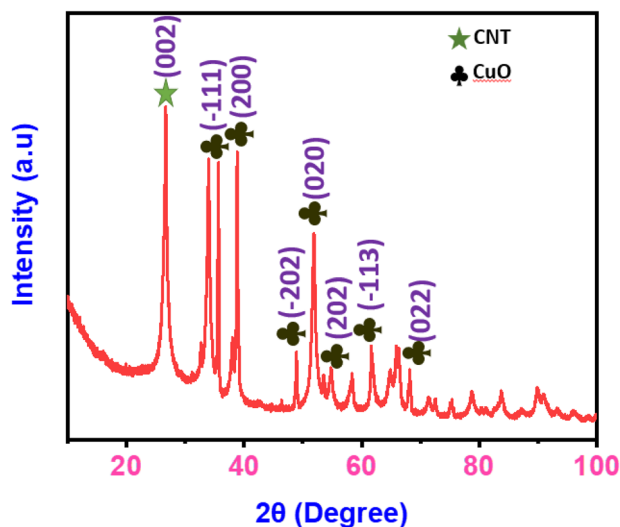


Figure 1. XRD pattern of CNTs-CuO NC. CNT, carbon nanotube; CuO, copper oxide; NC, nanocomposite; XRD, X-ray diffraction.

$2\theta = 35.4^\circ$ (–111), 38.8° (200), 48.7° (–202), 52° (020), 58.3° (202), 61.6° (–113), 65° (022), pertain to CuO nanoparticles (NPs) and were in good agreement with standard JCPDS card number 89-2531. CNT has a variety of orientations when compared to the X-ray incident beam. The distribution of diameters and chiralities of CNTs was also examined, resulting in statistical characterizations. Because of their intrinsic nature, the major characteristics of the XRD pattern of CNTs were identical to those of graphite. Peak (002), which has a graphite-like appearance, was also present. The cubic phase of CNT (JCPDS 26–1076) was also detected at $2\theta = 26.4^\circ$ (002), 43.0° (100), and $2 = 43.8^\circ$ (101), with these peaks matching to the inter-shell spacing of the concentric cylinders of graphitic carbon. According to diffraction investigations, the structure of as-prepared CNT was located between the chaotic amorphous carbon and highly organized graphitic phases.^[8] The crystallite size was calculated using the Debye–Scherrer equation.^[9] The study determined the average crystallite size of CNTs/CuO NC to be 30.95 nm. The diffraction peaks have expanded, showing that the NC was polycrystalline in its natural state.

The following is an inference of CNTs/CuO preparation. The bands at 1719 and 2439 cm^{-1} indicate that CNTs were functionalized with carboxylic and hydroxyl groups. When more $\text{NH}_3 \cdot \text{H}_2\text{O}$ was added, a complex $[\text{Cu}(\text{NH}_3)_4]^{2+}$ was produced. Through amide and carboxylic reactions, CNTs were linked to $[\text{Cu}(\text{NH}_3)_4]^{2+}$.^[10] No band corresponding to carboxylic groups can be identified in the FTIR spectra of CNTs/CuO NC, proving this. When NaOH solution was slowly added, $\text{Cu}(\text{OH})_2$ precipitate was formed in situ, and it was stabilized by chemisorption and van der Waals interactions between $\text{Cu}(\text{OH})_2$ and CNTs²¹. Under heating and stirring conditions, $\text{Cu}(\text{OH})_2$ was converted to CuO. During the synthesis of pure CuO NPs, the color of the solution changed from blue-green to blue, then black, which might assist confirm the above-mentioned CNTs/CuO production process to some extent. The useful vibration characteristics of the as-prepared NC were studied further. FTIR spectra in the range of $100\text{--}4000\text{ cm}^{-1}$ were collected under normal conditions. The

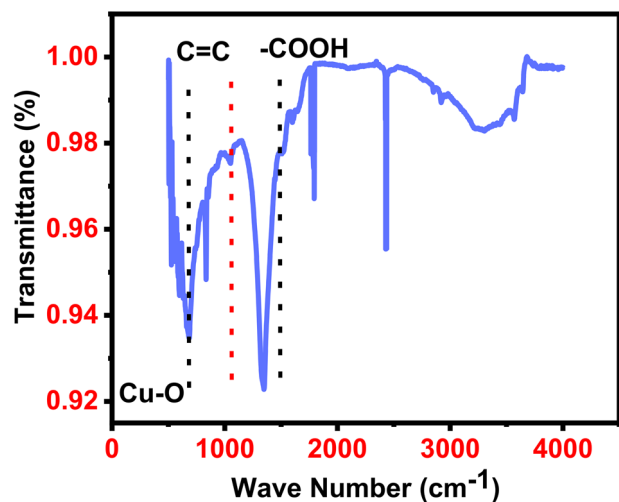


Figure 2. FTIR spectra of the prepared CNTs/CuO NC. CNT, carbon nanotube; CuO, copper oxide; FTIR, Fourier-transform infrared spectroscopy; NC, nanocomposite.

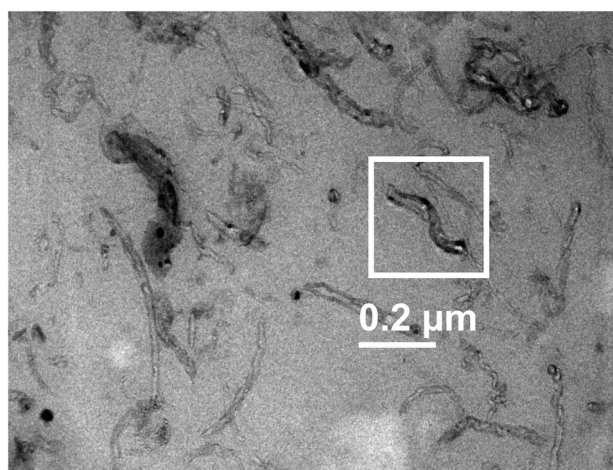


Figure 3. SEM image of CNTs/CuO NC. CNT, carbon nanotube; CuO, copper oxide; NC, nanocomposite; SEM, scanning electron microscopy.

vibrational bands in the FTIR spectra of CNTs-CuO are shown in **Figure 2**. The peak at 1479 cm^{-1} was caused by the O–H stretching mode. The C–O stretching vibration was attributed to the bands at 1386 cm^{-1} , while CO_2 physisorbed on the surface of the materials was attributed to the peak at 2458 cm^{-1} . In the absorption band at 523 cm^{-1} there was evidence of Cu–O bond bending. Furthermore, no impurity peaks were found in NC during XRD and FTIR analysis, showing that high purity CNTs/CuO NC was successfully synthesized using the complex-precipitation approach.

CuO NPs were very well spread over the CNTs surface in the SEM image of CNTs/CuO in **Figure 3**. The thickness of the loading layer and the homogenous dispersion of CuO NPs on CNTs were shown in this image. Despite the long-term sonication of the SEM specimen, faultless loading of CuO NPs on CNTs can still be seen, indicating the strong force between CuO NPs and CNTs.^[12] According to SEM images, the NPs were consistently generated, and the crystallite structure was uniformly or-

dered on the surface. The SEM image revealed the nanostructured characteristics of each particle. As seen in the SEM image, the nanoporous nature of the synthesized particles was also represented by the integration of NPs to generate the final micron-sized particles. The use of a surfactant in the synthesis process may have aided in creating nanoporous surfaces. The presence of holes in some of the particles indicates that they are hollow. As seen in the image, the porous morphology was evenly distributed over the CNTs/CuO NC surface. The presence of a porous structure on the surface of NC is advantageous since it improves surface permeability and adsorption efficiency. It also permits charge carriers to be transported quickly to the particle surface, reducing carrier recombination and speeding up surface reactions. The size of NC particles as-synthesized ranges from 30 to 100 nm. The results of the SEM match those of the XRD.

2.2. Electrochemical Profile of Acetone on CNTs/CuO NC

To test the efficacy of the CNTs/CuO NC customized GCE electrode, a CV experiment was performed in artificial sweat solution. **Figure 4** shows the electrochemical kinetics of the CNTs/CuO NC modified electrode for acetone detection using CV analysis. **Figure 4a** shows the CV curve for a CNTs/CuO NC modified electrode with and without 50 mM acetone at a scan rate of 100 mV s^{-1} . With an acetone-depleted electrolyte, there are no obvious redox peaks, as seen in **Figure 4a**. The current density of the CNTs/CuO NC modified electrode increases to 0.37 and -0.5 mA cm^{-2} at 0.15 and -0.16 V , respectively, in the presence of 50 mM acetone. Furthermore, in the presence of acetone, the CNTs/CuO NC modified electrode CV curves show improved current density and increased loop area. As shown in **Figure 4a**, acetone oxidation occurs at a lower potential,^[13] and the existence of a significant redox peak in the CNTs/CuO NC modified electrode supports the NC's high electrocatalytic performance for acetone detection. The oxidation peak retains its position regardless of scan rate modifications, as shown in **Figure 4b**.

Current density was explored further by plotting the cathodic and anodic peak current densities against the square root of scan rate (**Figure 4c**). Regardless of the oxidation or reduction cycle, the current density plot shows a linear relationship with the square root of scan rate. This indicates that the pace at which the electrolyte diffused to the active sites influenced the electrochemical processes. Furthermore, the linear relationship indicates that adsorption-controlled activity influenced acetone oxidation.^[5]

The electrochemical active surface area (EASA) of the CNTs-CuO NC catalyst was determined utilizing the scan rate dependency of CV studies shown in **Figure 4** and the CNTs-CuO NC catalyst's double-layer capacitance (Cdl) measurement. The Cdl was calculated by plotting the current density difference ($J = J_a - J_c$) between anodic and cathodic sweeps against the scan rate, as shown in **Figure 4d**. The Cdl of the CNTs-CuO NC catalyst was determined to be 19.5 mF cm^{-2} , showing a high density of the electrochemically active surface area because the fitted linear regression slope equals twice the Cdl. After that, the EASA was determined using the formula $\text{EASA} = \text{Cdl}/\text{Cs}$. On a unit surface area, Cs denotes the specific capacitance of conventional electrode materials. A typical Cs value of 0.02 mF cm^{-2} was employed in the computation, yielding in $\text{EASA} = 927$, according to

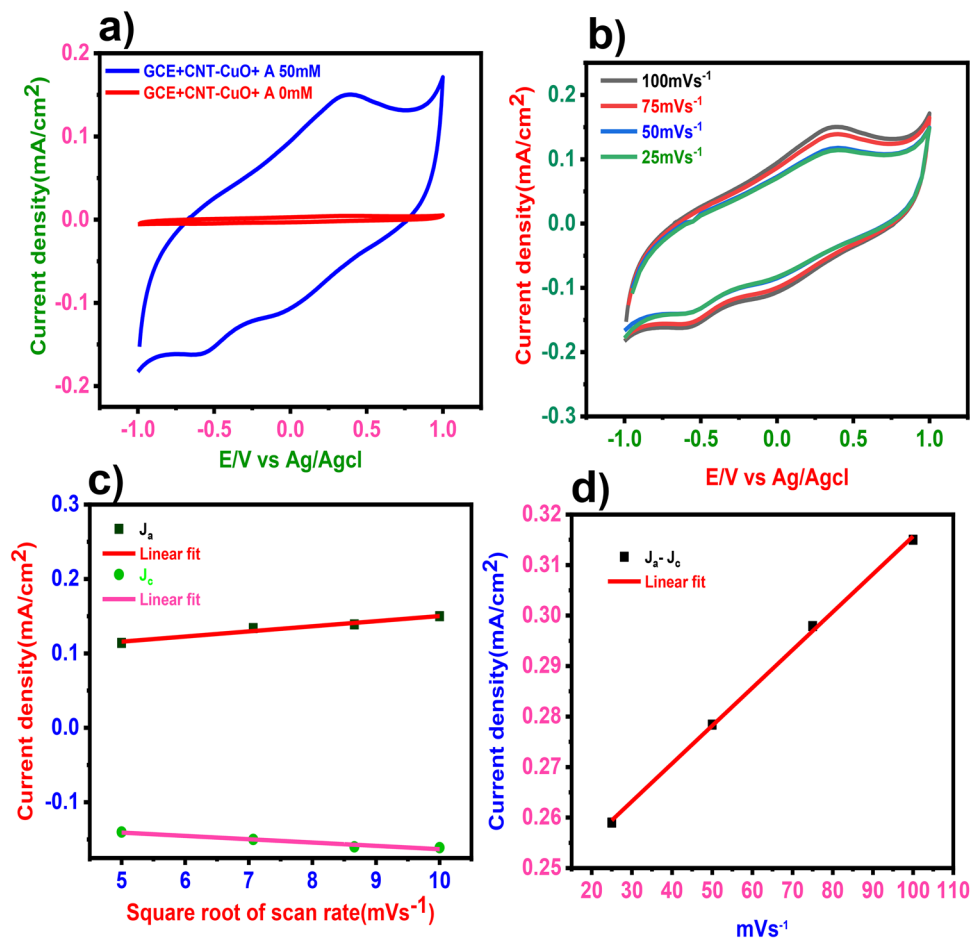


Figure 4. CV analysis of CNTs/CuO tailored GCE electrode. a) CV response of CNTs/CuO modified GCE electrodes with and without the presence of 50 mM acetone. b) CV measurement of CNTs/CuO tailored GCE electrode at different scan rates. c) Graph of redox peak current density with respect to the square root of scan rate. d) Linear fitting of the current density differences against scan rates. CNT, carbon nanotube; CuO, copper oxide; CV, cyclic voltammetry; GCE, glassy carbon electrode.

the literature.^[14] The calibration plot of the square root of scan rate and the peak current shows the modified electrodes' surface limited electrochemical redox process.

The sensitivity of the CNTs/CuO NC was further studied by altering the acetone concentration from 1 to 50 mM. Increased acetone concentrations were used to assess the concentration-dependent response of the produced CNTs-CuO NC on acetone (Figure 6). It was discovered that as the acetone concentration increased, the current increased as well. A linear trend with a positive slope and linear regression of 0.999 can be seen in the plot of concentration against the current density. This clearly shows that the oxidation process at the CNT-coated GCE is a surface-controlled phenomenon.

The $3\sigma/m$ criterion was used to compute the limit of detection (LOD), where m is the slope of the calibration plot and is the standard deviation of the intercept. Acetone LOD in the artificial sweat solution was estimated to be 0.05 mM ($y = (0.0153)x + (0.0149 \pm 0.00199)$). The sensor had a sensitivity of 16.1 mA cm⁻² μM⁻¹ and a response time of 2 s in a linear range of 1–50 mM. This implies that CNTs-CuO NC has a large surface

area and high conductivity, which boosts the electrocatalytic activity for acetone sensing in a synergistic manner.

One of the most important characteristics of sensing applications is its resilience to changes in the parameters of the surrounding or involved medium. The CV response of CNTs-CuO NCs in different pH sweat solutions (pH 3 [acidic], pH 7 [neutral], and pH 12) is shown in Figure 5c (alkaline). When acetone was added to pH 12, there was no significant change in current density. In the alkaline medium, the CNTs-CuO NC is stable for acetone detection, however, in the acidic and neutral solutions, no redox reaction occurs. When building a real-time biosensor implementation, it is crucial to consider the impact of temperature on sensitivity. Temperature impacts the performance of a CNTs-CuO NC electrode in a sweat solution, as shown in Figure 5d. As shown in Figure 5d, the CV curve exhibits a slight divergence in current density over a wide temperature range of 30 °C, 50 °C, and 100 °C. According to the research, temperature has no effect on the rate of redox pair reactions. According to the findings, the CNTs-CuO NC biosensor has good temperature stability, which is important for real-time acetone detection from human sweat.

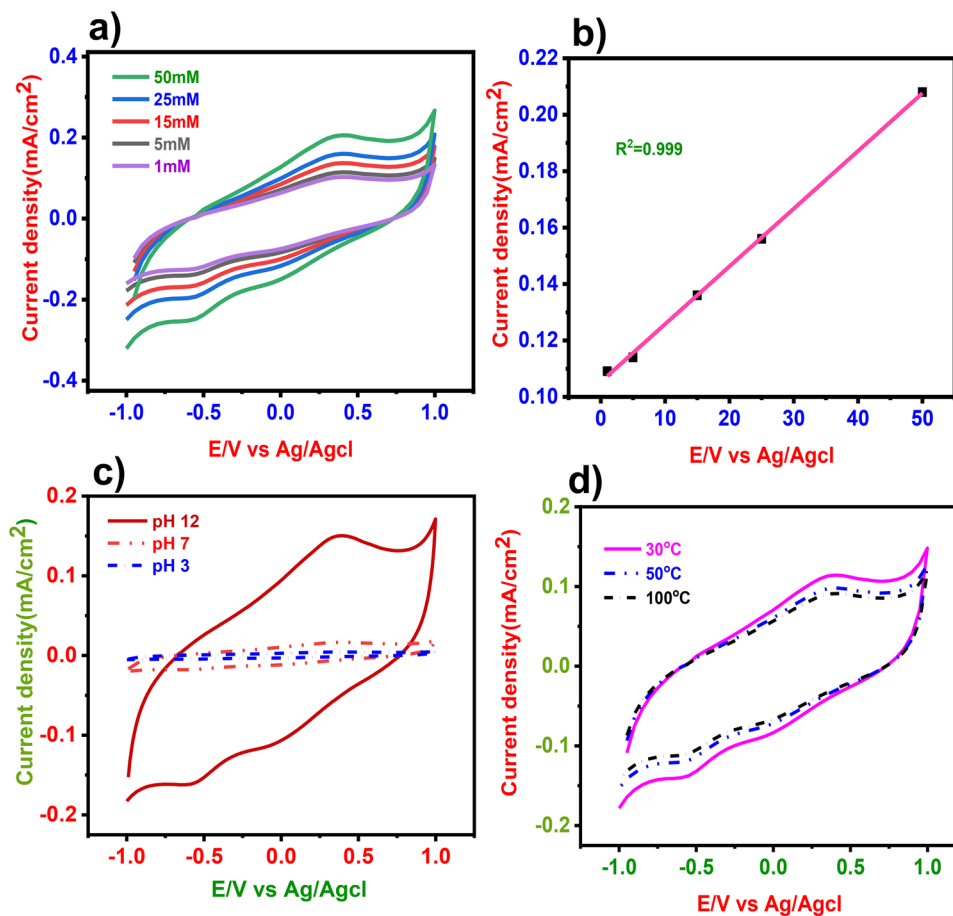


Figure 5. a) CV response of CNTs/CuO towards different acetone concentrations at a scan rate of 25 mV s^{-1} . b) The calibration curve in the linear range of 1–50 mM. c) The CV curve of CNTs-CuO NC at different pH levels. d) The CV plot of CNTs-CuO NC in pH 7 sweat solution at different temperatures. CNT, carbon nanotube; CuO, copper oxide; CV, cyclic voltammetry; NC, nanocomposite.

Selectivity, reproducibility, repeatability, and stability are all important characteristics to consider when evaluating sensing devices. Lactic acid, sucrose, fructose, uric acid, acetic acid, and ethanol are all easily oxidized compounds found in human perspiration with acetone. As a result, the selectivity of the CNTs-CuO NC is determined by amperometric measurement of various oxidizable compounds in response to acetone concentration, as shown in **Figure 6a**. Lactic acid, sucrose, fructose, uric acid, acetic acid, and ethanol do not create considerable interference, as seen in **Figure 6a**. As a result, the CNTs-CuO NC is highly selective for acetone detection instead of interacting with other species in the sweat. Repeatability is defined as the lack of incompatibility between subsequent readings taken with the same electrode. A single modified GCE was used three times in 1 day to verify the repeatability. The relative standard deviation (RSD) of the repeatability is 1.03%, as shown in **Figure 6b**, suggesting that the suggested sensor has outstanding repeatability.

Reproducibility refers to the similarity of results achieved using a number of the same modified electrodes and the same measuring technique. After each addition of 50 mM acetone, the CV responses of three independent electrodes were recorded under perfect conditions. The response currents' RSD for differ-

ent CNTs-CuO NC electrodes was just 1.45%, suggesting high consistency and accuracy (**Figure 6c**). To test long-term stability, the electrode response was examined in the presence of 50 mM acetone in artificial sweat solution at a scan rate of 100 mV s^{-1} . The suggested electrochemical sensor's durability was tested by storing the CNTs-CuO NC modified GCE electrodes in air and monitoring the current response. The response current of CNTs-CuO NC modified GCEs could be preserved at around 96.96% of its initial value after 15 days in the air, indicating good storage stability (**Figure 6d**). It takes a specific length of time from the moment the sensor is put to the electrolyte to achieve a steady state of sensor reactivity toward the substrate. It took 2 s for the sample to reach a steady current after being added to the sensor.

3. Conclusions

The current study used CNTs and CuO to demonstrate the nanocomposite's catalytic activity in detecting acetone in artificial sweat as an electrolyte. A thorough investigation of CNTs-CuO NC for acetone sensing was conducted. The CNTs-CuO NC was successfully made using the complex-precipitation approach. Because of its excellent electron transport properties,

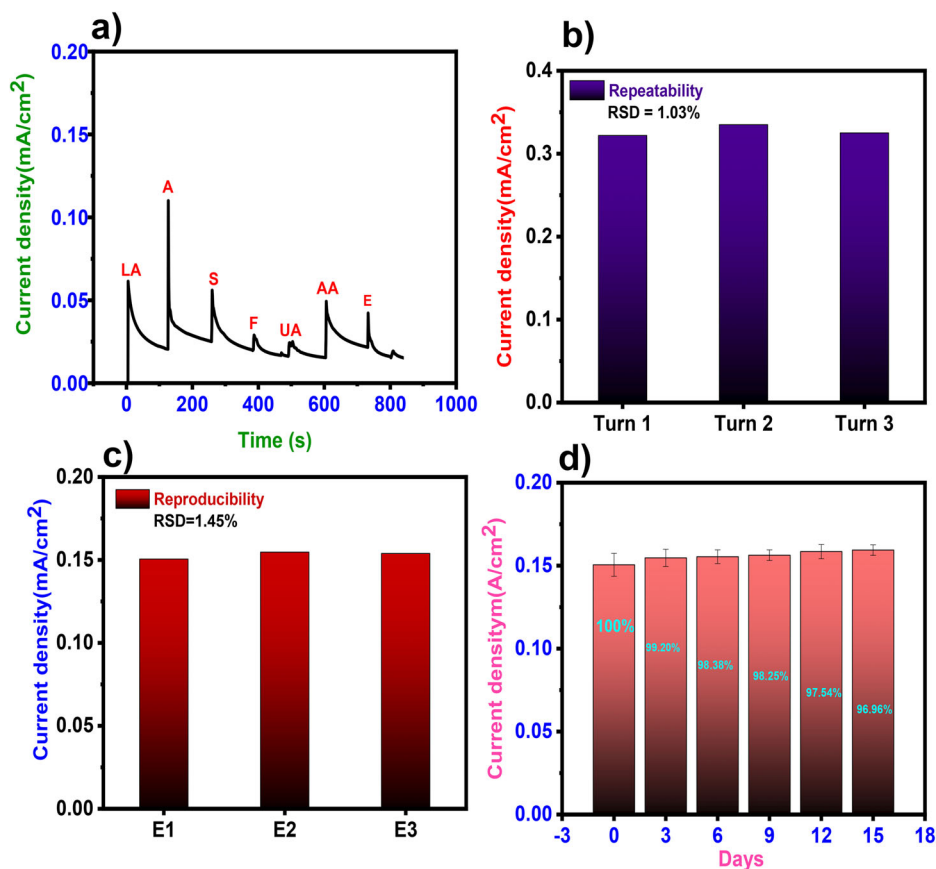


Figure 6. a) The chronoamperometric response of the CNTs-CuO NC sensor after the addition of 50 mM lactic acid, acetone, sucrose, fructose, uric acid, acetic acid, and ethanol in artificial sweat solution. b) Repeatability of the cyclic voltammetric analysis of CNTs-CuO NC sensor after addition of 50 mM acetone in artificial sweat solution. c) Reproducibility d) stability of the CNTs-CuO NC sensor after addition of 50 mM acetone in artificial sweat solution.

this NC developed a catalytic interface for successful electrochemical enzyme-free acetone detection. XRD confirmed the CNTs-CuO NC organization, with an average crystallite size of 30.95 nm. According to morphological examinations, the CNTs-CuO NCs with porous surfaces were homogeneous and well-defined. FTIR was used to establish the surface functional groups of CuO. CNTs-CuO NC acetone sensing capacity was tested using CV and chronoamperometry. The CNTs-CuO NC catalyst has a detection limit of 0.05 mM and a sensitivity of 16.1 mA cm⁻² M⁻¹ in the linear range of 1–50 mM, according to electrochemical studies. The CNTs-CuO NC offers good sensitivity, selectivity, quick response, and acetone detection stability in artificial sweat solutions. CNTs-CuO NC is a viable material to incorporate into wearable sensor devices for acetone sensing in the detection and control of diabetes risk, diabetic retinopathy, renal failure, and nerve degeneration due to its glucose-sensing properties.

4. Experimental Section

Materials: The study used acetone (Hi-media), Nafion (M/s Sigma-Aldrich Ltd), and CNTs (Nanomor, USA). M/s Sigma-Aldrich Ltd provided sodium dodecyl sulfate (SDS) and copper chloride (CuCl₂).

CH Instruments, Inc., USA, provided the glassy carbon electrode (GCE), KCl saturated Ag/AgCl reference electrode, and graphite rod counter electrodes for the electrochemical experiments. Scharlau provided the sodium hydroxide (NaOH, 98%). Fisher Scientific provided lactic acid (99%), ethanol (99%), uric acid (99%), ascorbic acid (99%), and fructose (99%). Sodium chloride was supplied by Avonchem (99%). Alfa Aesar provided urea (98%), lactic acid (85%–90% aqueous solution), potassium chloride (KCl, 99%), and ascorbic acid (99%). The experimental solutions were made with a solvent of double distilled water.

Synthesis of CNTs/CuO Nanocomposites (NC): A mixture of CNTs, SDS, and CuCl₂ was dissolved in 50 mL distilled water for 30 min. Additional aqueous ammonia(e) was subsequently added to the solution. Drop by drop, NaOH was added to the prepared solution and stirred at 50 °C for 1 h. After filtering, washing, and drying the sample with distilled water, it was calcined in a muffle furnace for 2 h.

Fabrication of CNTs/CuO Nanocomposites Modified Electrode and Artificial Sweat Solution: The catalytic ink was prepared by mixing 25 mg of CNTs/CuO NC with 0.5 mL of ethanol and 40 μL Nafion (proton conductor). Sonication on ice for an hour was performed on the resultant mixture. After ultrasonication, homogenized suspensions were dropped cast on GCE and dried at room temperature. In order to prepare the artificial sweat solution, 22 mM urea was added to 5.5 mM lactic acid, 25 mM uric acid, and 10 mM KCl¹⁶.

Characterization Techniques: Morphology and structure of the CNTs/CuO NCs were evaluated. An X-ray diffractometer (X'PERT-Pro MPD, PANalytical Co., Almelo, Netherlands) was used to study the crystal

structure. SEM and elemental mapping data were obtained using TESCAN Mira3. A thin layer of gold was sputter-coated on the sample and imaged at a 3 kV acceleration voltage. An FT-IR spectrum of KBr pellets was measured between 100 and 4000 cm^{-1} on a NicdeT 740 spectrometer to verify the chemical bonding. The CV and chronoamperometry tests were conducted using a three-electrode Gamry potentiostat/galvanostat (Ref 600). The counter, reference, and working electrodes were each 5 mm in diameter, and were comprised of graphite, Ag/AgCl, and GC solutions.

Acknowledgements

This publication was supported by Qatar University internal grant No. QUCG-CAM-21/22-1. The findings herein are solely the responsibility of the authors.

Conflict of Interest

The authors declare no conflict of interest.

Data Availability Statement

Data available on request from the authors.

Keywords

carbon nanotube, chronoamperometry, electrocatalysis, nanocomposite, sensors

Received: August 26, 2022

Revised: January 16, 2023

- [1] A. H. Jalal, F. Alam, S. Roychoudhury, Y. Umasankar, N. Pala, S. Bhansali, *ACS Sens.* **2018**, *3*, 1246.
- [2] Y. Obeidat, *IEEE Sens. J.* **2021**, *21*, 14540.
- [3] S. Singh, A. Numan, S. Cinti, *Anal. Chem.* **2022**, *94*, 26.
- [4] G. Bepete, K. S. Coleman, *Comprehensive Nanoscience and Nanotechnology*, **2019**, p. 205.
- [5] R. Zarrin, R. E. Emamali Sabzi, *Anal. Bioanal. Chem. Res.* **2022**, *9*, 113.
- [6] A. Jahangiri-Manesh, M. Mousazadeh, M. Nikkhah, *Iran. Polym. J.* **2022**, *31*, 883.
- [7] A. H. Jalal, Y. Umasankar, M. Chowdhury, S. Bhansali, *ECS Trans.* **2017**, *80*, 1369.
- [8] K. Lin, H. Fang, F. Wen, L. Wang, W. Jiang, J. Li, *Carbon* **2019**, *149*, 436.
- [9] S. Mustapha, M. M. Ndamitso, A. S. Abdulkareem, J. O. Tijani, D. T. Shuaib, A. K. Mohammed, A. Sumaila, *Adv. Nat. Sci.: Nanosci. Nanotechnol* **2019**, *10*, 045013.
- [10] F. Limosani, E. M. Bauer, D. Cecchetti, S. Biagioni, V. Orlando, R. Pizzoferrato, P. Proposito, M. Carbone, *Nanomaterials* **2021**, *11*, 2249.
- [11] M. Farouk, K. Abdallauh, M. Attallah, Z. M. Abd El-Fattah, *J. Non-Cryst. Solids* **2019**, *523*, 119607.
- [12] V. Soni, P. Singh, A. A. P. Khan, A. Singh, A. K. Nadda, C. M. Hussain, Q. Van Le, S. Rizevsky, V. H. Nguyen, P. Raizada, *J. Nanostructure Chem.* **2023**, *13*, 129.
- [13] J. Kaur, K. Anand, K. Anand, R. C. Singh, *J. Mater. Sci.* **2018**, *53*, 12894.
- [14] F. Wang, X. Sun, Y. Wang, H. Zhou, J. Yin, X. Zhang, Metallized Ni (OH)₂ NiO/FeOOH on Ni foam as Highly Effective Water Oxidation Catalyst Prepared by Surface Treatment: Oxidation-Corrosion Equilibrium.